Flexible and Transparent Surface Enhanced Raman Scattering (SERS)-Active Ag NPs/PDMS Composites for *in-situ* Detection of Food Contaminants

Abeer Alyami, Aidan J. Quinn and Daniela Iacopino*

Tyndall National Institute, University College Cork, Dyke Parade, Cork, Ireland

*Email: daniela.iacopino@tyndall.ie

Abstract

The fabrication of flexible and transparent Surface Enhanced Raman Scattering (SERS) substrates enabling fast, sensitive and on site detection is relevant for the practical application of SERS for real world analysis, such as food safety and organic pollutants monitoring. In this work novel Ag NPs/PDMS composites were fabricated and exmployed for the SERS detection of food contaminants directly on food surfaces. Ag NPs/PDMS composites were obtained by self-assembly of organic Ag nanoparticle solutions on flexible PDMS surfaces. Preliminary evaluation of the suitability of Ag NPs/PDMS probes for SERS analysis showed that ocomposites were characterised by a SERS enhancement factor (EF) of 3.1×10^{5}, good stability and resistance to harsh conditions as well as good uniformity and batch to bach reproducibility. The "sticky" nature of Ag NPs/PDMS composites was exploited to "paste" them on irregular analytical surfaces, thus enabling the detection *in situ* of food contaminant crystal violet (CV) and pesticide thiram, respectively. Specifically, CV and thiram concentrations as low as 1×10^{-7} M and 1×10^{-5} M were measured on contaminated fish skin and orange peel, respectively. Furthermore, efficient SERS detection by micro-extraction of CV from fish skin and thiram from

fruit surfaces was achieved, showing the analytical versatility of the fabricated SERS composites.

Keywords: SERS, food contaminants, composites, pesticides, flexible, transparent.

Introduction

Surface Enhanced Raman Scattering (SERS) has become an established and powerful analytical technique, due to its effectivness for ultrasensitive detection, arising from the combination of Raman spectroscopy's fingerprinting ability and plasmonic-enabled enhanced sensitivity [1,2]. In the last twenty years much effort has been devoted to the development of methodologies for the ordered assembly of plasmonic structures on rigid substrates (SiO_2, glass, quartz) [3-5], in order to burst SERS sensitivity and reproducibility of analysis. However, the implementation of such rigid SERS substrates has been often impractical, due to the need of extraction procedures and high cost of production. It is now recognised that a combination of cost-effective fabrication routes with high sensitivity, reproducibility and versatility of analysis is desirable to widen the SERS range of applications to practical detection systems for routine or field analysis [6]. Consequently, the focus of recent research has shifted towards development of alternative fabrication routes, whereby flexible surfaces such as plastic [7-9], paper [10-12] and polymer materials [13,14] have been used as support. The deposition of the plasmonic SERS-active layer is usually obtained by solution-based fabrication processes, which offer fine control over the size and shape of deposited nanoparticles and are compatible with scalable fabrication methods such as printing [15] and dip-coating [16]. As well as being cost–effective and offering high sensitivity useful for routine analysis, flexible

substrates have widened the range of SERS applications, due to their increased sampling versatility (swabbing, microextraction etc.) [17,18].

The field of food safety/monitoring could particularly benefit from the development of low-cost SERS probes. Food chemical contaminants are primarily of agricultural origin (pesticides) and environmental (chemical adulterants) and are currently detected effectively by mass spectroscopy and chromatography techniques [19,20]. However, the repeated occurrence of food scandals calls for development of lower cost, accurate and fast methods with *on site* measurement capabilities. Recently, this goal was achieved with the development of flexible and transparent SERS substrates, which enabled contamination-free *in situ* analysis directly on irregular objects without the need for invasive and cumbersome solvent extraction techniques. By using flexible transparent SERS substrates, Zhong *et al.* detected model molecule malachite green on fish surface by deposition of an Au nanoparticle/PMMA composite directly on the contaminated fish skin [21] Chen *et al.* used transparent Au NP/adhesive tape to detected pesticide residues on fruit and vegetable peels [22]. Organic pollutants such as methyl parathion were measured on orange skin by deposition of Ag nanocrystals/polyethylene films (Ag NC@PE films) [23]. However, the adhesion of developed substrates on irregular surfaces was not optimal as Au NP/PMMA substrates had to be wet in order to ensure full adhesion with the fish skin and Ag NC@PE films had to be fixed with band aid strips in order to promote close contact with the analytical surface. In contrast, the use of polymethylsiloxane (PDMS) as support in combination with Au nanostars proposed by Shiohara *et al.* resulted in fabrication of macroscale highly sensitive SERS substrates with controllable thickness and good adhesion to fruit surfaces [24] Interestingly, the authors used anisotropic particles as in their opinion spherical particles would provide SERS signals too low for the targeted application.

In this paper we report the fabrication of SERS substrates obtained by self-assembly of spherical Ag NP organic solutions into PDMS substrates. The SERS capabilities of obtained Ag NPs/PDMS composite films were tested with model molecule 4-ABT. Concentrations down to 1×10^{-9} M were measured, leading to EF of 3.1×10^{5}. As well as sensitivity, 4-ABT was used to investigate uniformity, batch to batch reproducibility, stability and resistance to harsh conditions in order to determine the suitability of SERS composites for real life applications. The transparency of PDMS was exploited to detect crystal violet (CV) residues on fish skin and thiaram on orange peel by *in situ* SERS back illumination. The controllable thickness of PDMS was exploited to ensure that no competitive signals from PDMS were obtained during analysis. The "sticky" nature of PDMS ensured that good adhesion of Ag NPs/PDMS composite films was obtained on the analytical irregular surfaces. Detection of concentrations as low as 1×10^{-7} M and 1×10^{-5} M was achieved for CV and thiram, respectively. Furthermore, CV and thiram could also be detected directly on Ag NPs/PDMS composite surfaces following micro-extraction from contaminated fish skin and fruit peels.

Materials and Methods

Silver nitrate, sodium borohydride,trisodium citrate, octadecylamine (ODA), chlorobenzene, methanol, ethanol, Crystal violet (CV), 4-aminobenzenethiol (4-ABT) and thiram were purchased from Sigma-Aldrich used without further purification. SYLGARD 184 Silicon Elastomer Kit for polydimethylsiloxane (PDMS) film fabrication was also purchased from Sigma-Aldrich. All glassware was cleaned with *aqua regia* prior to silver nanoparticles synthesis. Milli-Q water (resistivity 418 MΩ/cm) was used throughout the experiments. Fish and organic fruits were bought from the local market and rinsed with deionized water before SERS analysis.

Synthetic procedures

Ag NPs were synthesized according to a process reported previously by Rainville *et al*. [25]. Briefly, 12 mL of an aqueous solution (0.2% w:w) of silver nitrate and 488 mL of deionized water were mixed and heated to 100 °C. Next, 11.6 ml of an aqueous solution of sodium citrate (3.4×10^{-2} M) was added, followed 30 s later by the quick injection of 5.5 mL of a freshly prepared, ice-cold aqueous solution of sodium borohydride (0.2 M) and sodium citrate (0.03 M, 50 mL). The solution was stirred for 2 min and subsequently left it to cool at room temperature. The obtained nanoparticle solution was centrifuged once at 9000 rpm for 20 mins and redispersed in 4 ml of distilled water. The concentrated NP solution was stored in the dark for subsequent use.

Ag NPs were transferred to organic phase by slight modification of a method previously reported [26]. Briefly, 2 mL of the concentrated aqueous Ag NP solution were added to 2 mL of a 2×10-5 M solution of ODA in chlorobenzene. The two solutions were vigorously stirred for 60 mins to facilitate the transfer of Ag NPs to the organic phase.

PDMS was fabricated by pouring 10:1 (w:w) of Sylgard 184 elastomer and curing agent in a petri dish followed by heating at 60 °C for 24 hrs. After removal from oven, the PDMS film was rinsed with isopropanol several times, dried with nitrogen gun and cut to small squares of 1×1 cm. The final thickness of the PDMS film was 1 mm.

In order to obtain Ag NPs/PDMS composites, a small aliquot (10 μL) of Ag NP chlorobenzene solution was deposited on an acetone- cleaned glass coverslip. The droplet was left in contact with air (5 min) until Ag NPs spontaneously self-assembled at the solvent/air interface, as shown by the formation of a metallic lustre layer. A flexible transparent PDMS film was used as support to retrieve the assembled NPs by bringing it

into contact with the NP droplet for 30 s. Excess organic matter was removed by immersing the Ag/PDMS composite in isopropanol overnight, followed by multiple rinses with fresh isopropanol.

Characterisation

UV-vis spectra were acquired using an Agilent/HP 8453 UV-vis Spectrophotometer (200 nm to 1100 nm). Scanning electron microscopy (SEM) images of Ag NPs and Ag NPs/PDMS composite films were acquired using a field emission (JSM- 6700F, JEOL UK Ltd.) scanning microscope operating at 3 kV.

Raman and SERS measurements were obtained from a Renishaw inVia Raman system equipped with a 514 helium–neon laser. The laser beam was focused onto the sample through a Leica 20X objective with 0.4 N.A. Acquisition time was usually 10 s and measured power was 3 mW.

For SERS sensitivity measurements, 10 μL of aqueous 4-ABT solutions of different concentrations (ranging from 1×10^{-4} to 1×10^{-9} M) were deposited onto clean glass slides and left to evaporate at room temperature. An Ag NPs/PDMS film (1×1 cm) was pressed on the glass slide with the Ag NPs side in contact with the dried 4-ABT. SERS signals directly were collected by back illumination of the Ag NPs/PDMS composite film.

Uniformity data were acquired by measuring SERS signals from five different areas of an Ag NPs/PDMS composite film deposited on a glass slide containing dried 4-ABT droplets (obtained by evaporation of 1×10^{-4} M 4-ABT solutions). For batch to batch reproducibility analysis, SERS signals were collected from five different composite films deposited on evaporated 4-ABT droplets. Time stability assessment was performed by depositing an Ag NPs/PDMS composite film on dried 4-ABT droplets and measuring

SERS spectra over a three month period. Resistance to harsh condition assessment was carried out by measuring 4-ABT spectra before and after immersion of Ag/PDMS composite films to NaOH 1 M for 1hr, HCl 1 M for 1hr, boiling water for 1 hr.

For CV detection fish skin samples (1×2 cm) were immersed in CV solutions (EtOH) of different concentration ranging from 1×10^{-5} to 1×10^{-7} M for 10 min, then dried at room temperature. Ag NPs/PDMS composite films were placed on the dried fish skin with the Ag NP side facing the CV-contaminated fish surface for backside SERS measurements. Alternatively, CV micro-extraction was performed by pressing the Ag NPs/PDMS composite film against the CV-contaminated fish skin for 10 s, followed composite removal and front SERS illumination.

For detection of thiram trace, thin peels (1×2 cm) of orange skin were cut and contaminated by deposition of 0.01mM thiram droplets (EtOH, 10 μL). Ag NPs/PDMS composite film was deposited on the contaminated orange peel and backside SERS measurements performed. Alternatively, SERS was performed on micro-extracted thiram obtained by pressing the Ag NPs/PDMS composite film on thiram-contaminated orange and apple peels for 10 s. SERS measurements were subsequently performed on the front side of the removed SERS substrate.

Results and discussion

Ag NPs used in this study were prepared with a method developed by Rainville *et al.* [25]. Ag NPs showed an average size of 15 nm (see Figure S1a). The concentration of obtained NPs was increased by two orders of magnitude by centrifugation and subsequent re-dispersion in 4 ml of deionized water. This step was necessary to promote the subsequent assembly of NP organic solutions at the air/solvent interface. The fabrication

of Ag NPs/PDMS composite films is shown in Scheme 1. First of all (Scheme 1a.1), concentrated NPs were phase-transferred from water to chlorobenzene by surface modification with ODA. The transfer process took place at pH 8.4 and was likely promoted by the formation of a coordination bond between the amine groups of ODA and the surfaces of the Ag NPs, as reported by Sastry *et al.* [27]. Photographs of the process (b,1) showed that complete discoloration of the aqueous phase did not occur and that therefore not all particles transferred successfully to organic phase. However, the concentration of transferred particles was high enough to promote their subsequent self-assembly in organic phase, as shown by the formation of a metallic layer on the wall of the glass container. In order to promote self-assembly at the air/solvent interfase, a droplet deposition method was followed (a2) whereby 10 μL of Ag NP organic solution were deposited on a glass coverslip and left exposed to air for 5 min. The quick occurring of a self-assembly process was clearly visible from the formation of a superficial metallic layer, attributed to the optical coupling of the densely packed Ag NPs (b2). A transfer process followed (1c) whereby a thin PDMS film was brought in contact with the Ag NP metallic layer for 30 sec, which caused the transfer and subsequent attachment of the Ag NP layer to the organic film (a,3). Excess organic solvent and ODA residues were washed away by overnight immersion of the resulting Ag NPs/PDMS composite film in isopropanol (b,3). PDMS was selected as support for its chemical inertness, non-toxicity and transparency. In addition, its tunable shape size and thickness as well as its "stickiness" were highly desirable features for the targeted application of *in situ* food quality monitoring as they enabled effective coverage of arbitrary surface samples while

allowing plasmon interaction with the analytical surface and hence effective collection of SERS signals.

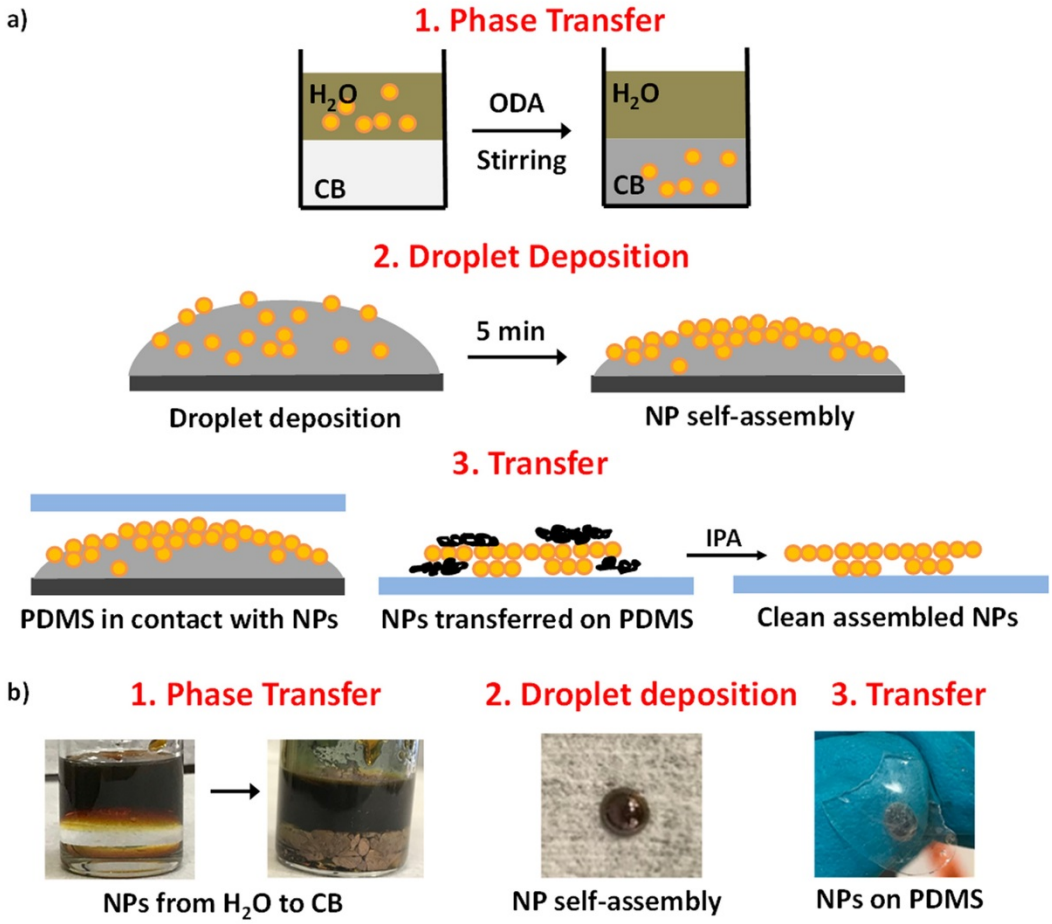

Scheme 1: a) schematic representations of phase transfer, droplet deposition and transfer processes; b) representative photographs illustrating the same processes depicted in a).

Figure 1a (black line) shows the UV-vis spectrum of Ag NPs as synthesized in aqueous solution. The NPs were characterized by a band centered at 388 nm and a shoulder at 425 nm. The spectrum of the Ag NPs/PDMS composite, also shown in Figure 1a (red line), was characterized by a broad band from 420 to 800 nm, ascribed to the plasmonic coupling between neighboring Ag NPs. A SEM image of the Ag NP layers transferred on

the PDMS film is displayed in Figure 1b. Dense and high coverage of surface areas larger than 10 μm^2 was achieved. Closer observation of magnified areas (Figure 1c) showed that multilayers formed during the process. The high resolution SEM inset of Figure 1c confirms that nanoparticle size and shape was maintained during the phase transfer and subsequent attachment to PDMS supports. A number of factors were considered responsible for the self-assembly of Ag NPs in chlorobenzene and their transfer to PDMS: i) lower surface tension of chlorobenzene compared to the original water solvent, which promoted movement of particles close to each other and therefore self-assembly; ii) formation of a well-defined and high curvature droplet, due to the high contact angle of chlorobenzene on glass; iii) strong Wan der Waals hydrophobic attractive forces between ODA alkyl chains which overcame electrostatic forces between nanoparticles; iv) affinity between hydrophobic PDMS and assembled organic Ag NPs, which promoted adhesion of transferred particles to the host substrate.

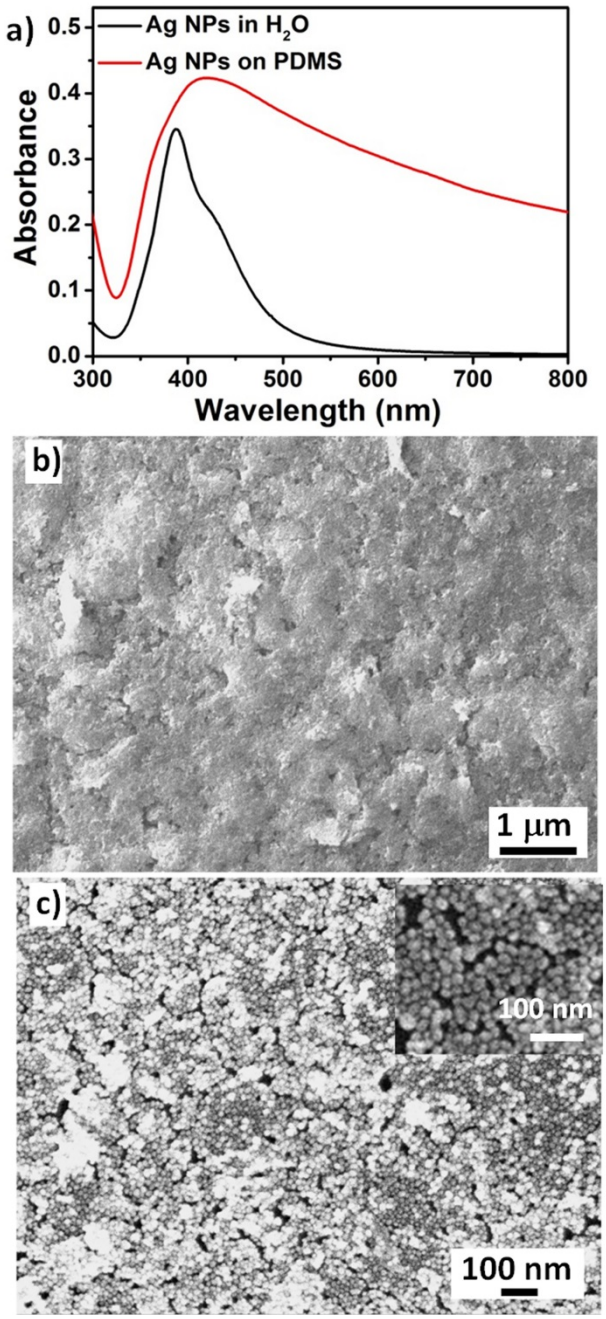

Figure 1: a) UV-Vis spectra of Ag NPs aqueous solution (black line) and Ag NPs/PDMS composite film; b) low resolution SEM image of Ag NPs transferred on PDMS film; c) high resolution SEM image of Ag NPs/PDMS film. Inset: SEM image of a portion of Ag NPs/PDMS film showing morphology of individual transferred NPs.

To evaluate the SERS sensitivity of the Ag NPs/PDMS composites, samples were prepared by placing a composite film on dried drop-cast 4-ABT solutions of different concentrations ranging from 1×10^{-4} to 1×10^{-9} M. The Ag NP side of the composite faced the dried 4-ABT droplets and SERS measurements were taken by backside direct illumination of the Ag NPs/PDMS films in contact with the analytical surface.

Figure 2 shows SERS spectra obtained for 4-ABT films with concentrations ranging from 1×10^{-4} to 1×10^{-9} M. All spectra showed clear signatures of 4-ABT with bands centered at 1077, 1142, 1471 and 1576 cm^{-1} associated with the a_1 vibrational, in plane, in phase modes of 4-ABT [28]. In addition to a_1 bands, SERS spectra showed b_2 in plane, out of phase vibrational modes at 1190, 1390 and 1433 cm^{-1}. The formation of b_2 peaks has been observed in SERS spectra of 4-ABT recorded on nanostructured surfaces and has been attributed to a metal-molecule charge transfer related to a chemical enhancement process [29,30]. The clear features showed by the SERS spectrum obtained at the lowest concentration of 1×10^{-9} M suggested that even lower concentrations could be measured with the fabricated composite films.

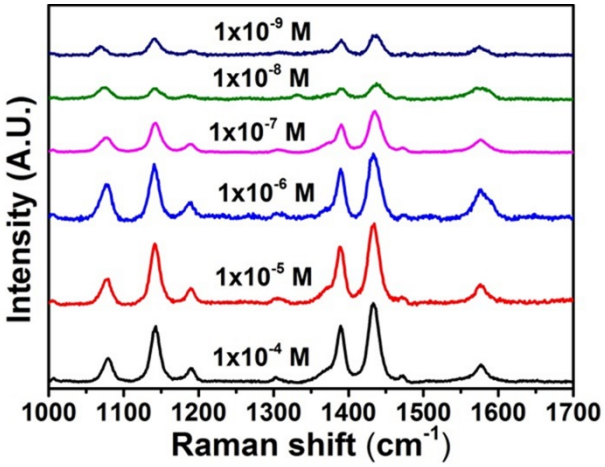

Figure 2. SERS spectra of 4-ABT with different concentrations from 1×10-4 to 1×10-9 M obtained by back illumination of Ag NPs/PDMS composite film at excitation wavelength of 514 nm.

Assessment of signal uniformity achievable with these composites was carried out by taking five intensity measurements of the 1077 cm^{-1} signal over an area of 100×100 μm of the composite film in contact with 4-ABT. A relative standard deviation (RSD) of 13% (see Figure S2,a) was obtained, in line or lower than values reported for similar SERS substrates [21-23]. Furthermore, batch-to-batch reproducibility was assessed by measuring 4-ABT signal intensity variations (at 1077 cm^{-1}) over five Ag NPs/PDMS composite composites, which yield to an RDS of 8%, as reported in Figure S2,b.

To further evaluate SERS performances of the fabricated SERS composite films, the enhancement factor (EF) was calculated following the following equation:

$EF= (I_{SERS}/N_{SERS})/(I_{Raman}/N_{Raman})$

where I_{SERS} and I_{Raman} are the integrated of the SERS and Raman scattering spectra for 4-ABT, respectively. N_{SERS} and N_{Raman} denote the number of 4-ABT molecules found in the laser excitation area adsorbed on the composite film and in bulk form, respectively. For calculation the intensity of the 4-ABT band at 1077 cm^{-1} was used. The SERS EF of Ag NPs/PDMS film was calculated equal to 3.1 $\times 10^5$ (see SI for details). This value was in line with values obtained for similar flexible substrates [21-23].

Ag NPs/PDMS composite films were further tested to investigate their suitability for real world applications. Towards this end, the estimation of signal stability of over time was investigated. An Ag NPs/PDMS film was placed on a dried 4-ABT droplet (10^{-5} M) on a

glass slide and SERS spectra were measured by back-illumination of the composite film. Spectra of the same sample were also measured after been stored in the dark for three months. Measured spectra at time zero and three months are reported in Figure S3,a, showing good reproducibility of recorded spectra. Resistance to harsh conditions was also tested by comparing SERS spectra of drop-deposited 4-ABT taken with freshly made composite films and with films immersed in HCl 1M, NaOH 1M and boiling water. In all cases only slight variations in spectral intensity were recorded, as clearly shown in Figure S3b-c.

In order to evaluate the applicability of Ag NPs/PDMS composite films for environmental monitoring applications, a test of residual food contaminants was carried out. Crystal violet (CV) is a toxic cationic dye largely used as food colouring agent and food additive. CV has also being used illegally to improve the survival rate of fish in water body [31]. CV has been classified as recalcitrant molecule since it is poorly metabolized by microbes, is not bio-degradable and can persist in a number of environments. For these reasons the minimum required performance limit (MPRL) was set for 2 mg L^{-1} (ca. 4.9 nM) in European Commission and US [32].

Figure 3b shows spectra of CV measured *in situ* on fish skin by deposition of an Ag NPs/PDMS film on the contaminated skin followed by SERS back illumination. Spectra were recorded at different CV concentrations from 1×10^{-5} to 1×10^{-7} M. Vibrational bands of CV appeared at 1619, 1587, 1390 and 1175 cm^{-1} and were associated to the stretching of the benzene rings [33]. Figure 3c shows the SERS enhancement obtained on CV-contaminated fish skin compared to simple Raman conditions. For fish skin samples contaminated with 1×10^{-5} M CV, the Raman spectrum appeared featureless, whereas

SERS spectra showed intense features, suggesting that enhancements up to 4 orders of magnitude can be achieved with the use of composite films.

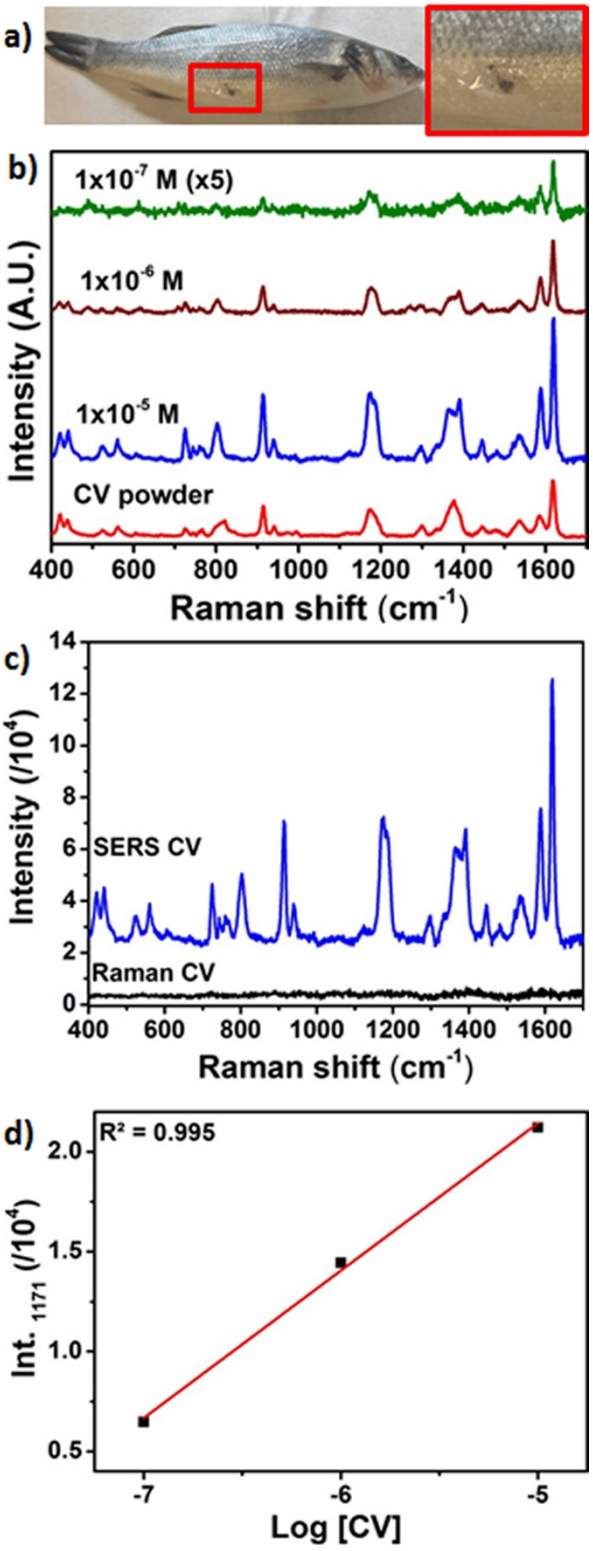

Figure 3: a) Photograph of fish with pasted Ag NPs/PDMS composite film; b) SERS spectra of CV at different concentration from 1×10^{-5} to 1×10^{-7} M recorded by direct deposition of Ag NPs/PDMS composite films on fish skin; c) Comparison between Raman and SERS spectra of CV 1×10^{-5} M on fish skin. All spectra were recorded at 514 nm illumination wavelength; d) plot of CV SERS intensity measured at 1171 cm^{-1} peak against CV concentration of fish surface.

Figure 4d shows the peak intensities of the 1171 cm –1 CV band as a function of the logarithmic concentration of CV displaying good linear correlation. It should be pointed out that no further supports (tapes etc.) were used to keep the Ag NPs/PDMS composite in place during analysis. The composites used are constituted by a 25 mm^2 square with a spherical drop of Ag NPs of 5 mm diameter in the middle. The good adhesion of the composite to the analytical surface is ensured by the large surface of PDMS not covered with Ag NPs, which adheres to the analytical surface and promotes close contact between the entire composite and the analytical surface.

In addition, the applicability of fabricated SERS composites for detection of pesticides on fruit was tested. Thiram, a dithiocarbammate compound, is widely used as a fungicide in agriculture and a bactericide in medical treatment [34]. Figure 4a shows spectrum (red line) of orange peel obtained by deposition of Ag NPs/PDMS composite film followed by back SERS illumination. The spectrum was dominated by strong bands at 1528, 1189, 1157 and 1005 cm^{-1} associated to the high content of vitamin C in the orange peel [35] However, the spectra of orange peel exposed to thiram 1×10^{-4} to 1×10^{-5} M solutions (green and blue lines) showed an additional week band centered at 1384 cm^{-1}, associated

to thiram C-N stretching and CH_3 deformation [36]. Figure 4b shows the direct comparison between Raman and SERS spectra recorded on orange peel spiked with 1×10^{-4} M thiram, highlighting the superior sensitivity of the latter by two orders of magnitude.

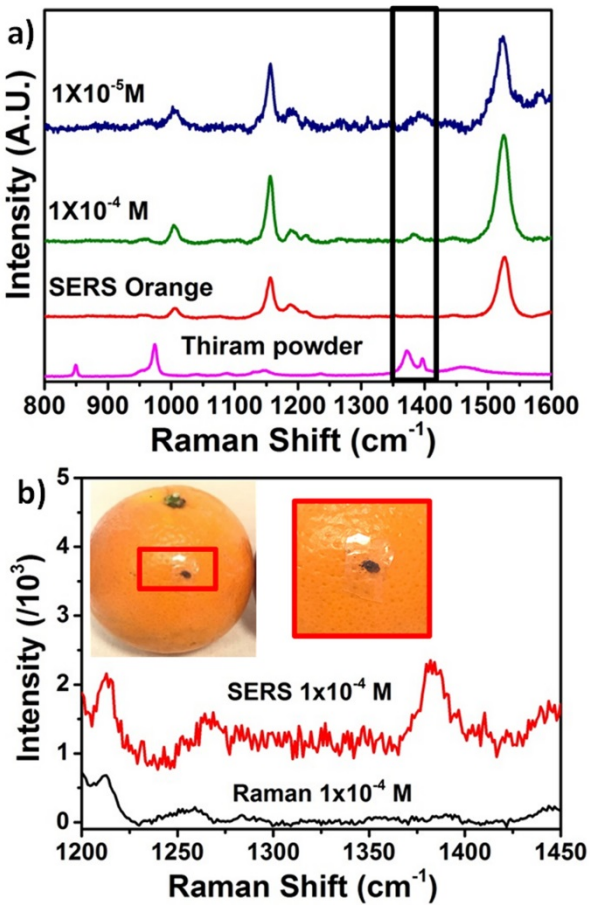

Figure 4: a) SERS spectra recorded for orange peel (red line) and orange peel treated with 1×10^{-4} and 1×10^{-5} M thiram (green and blue spectra). All SERS were recorded by direct deposition of Ag NPs/PDMS composite film on orange peel; b) SERS and Raman spectra of thiram 1×10^{-4} M deposited on orange peel and Raman spectrum of reference bulk thiram. All spectra were obtained at 514 nm illumination wavelength.

The SERS ability of composite films for analysis of food contaminants in real complex matrices was also tested by extraction of target analytes, which was promoted by the

"sticky" nature of the PDMS support. First of all, micro-extraction was performed on CV-contaminated fish skin. In order to perform measurements, fish skin samples were immersed for 10 min in CV solutions of different concentrations between 1×10^{-5} and 1×10^{-7} M. Ag NPs/PDMS films were placed on the fish skin with the Ag NP side facing the skin and left in contact with the analytical surface for few seconds to promote micro-extraction. SERS spectra recorded on micro-extracted CV are shown in Figure 5a. Spectra showed characteristic bands of CV at 1619, 1587, 1390 and 1175 cm^{-1}. Sensitivities comparable to those obtained by direct back illumination (Figure 3a) were obtained for the same investigated concentration range. Same experiments were carried out on fruit peels in order to demonstrate detection of thiram. Figure 5,b shows SERS spectra obtained for orange peel spiked with 1×10^{-4} M thiram solution. In contrast with the weak spectral signatures obtained with the direct method described in Figure 4, clearer bands attributable to thiram were obtained by micro-extraction. Specifically, the spectrum of Figure 5b was characterized by bands at 1381 (C-N stretching and CH_3 deformation), 1146 (C-N stretching) and 562 cm^{-1} (S-S stretching). The clearer detection of thiram obtained by micro-extraction compared to direct measurements was attributed to the exclusion of the vitamin C contribution in the latter case. The detection of thiram on apple peel is also shown in Figure 5c, displaying clear thiram spectral signatures down to 1×10^{-5} M, below the maximum residual limit (MRL) set for this pesticide [37].

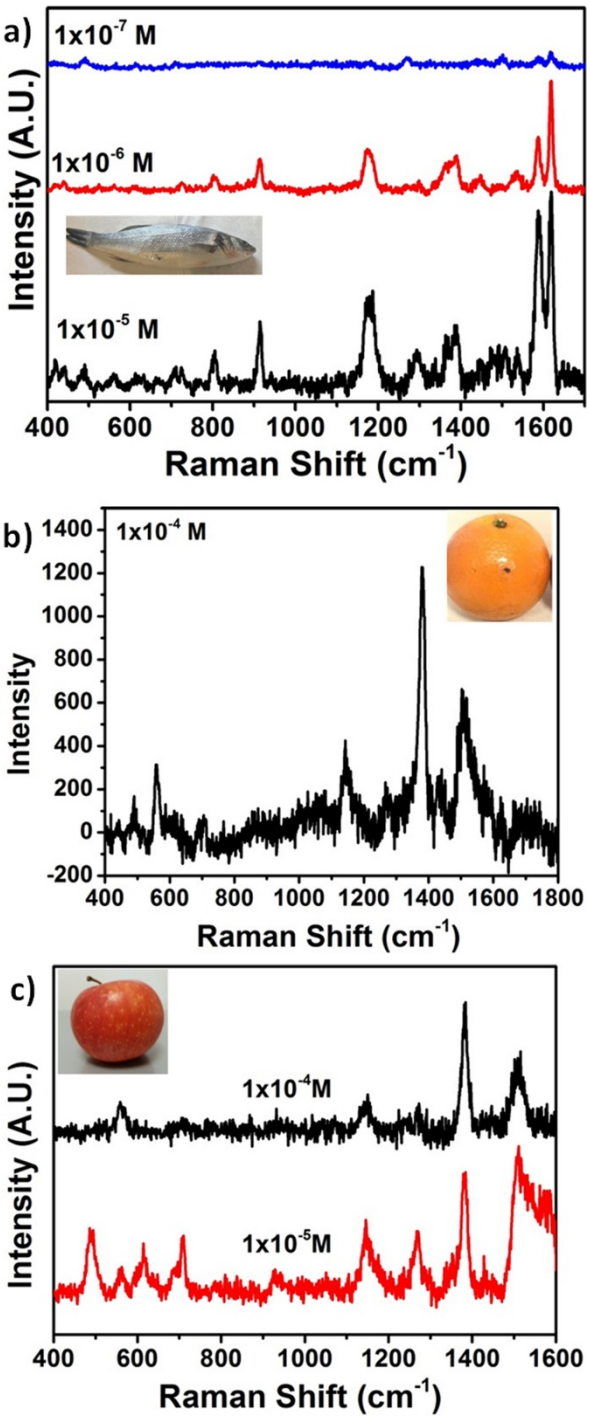

Figure 5: a) SERS spectra of CV extracted from fish skin in the 1×10^{-5} to 1×10^{-7} M concentration range using Ag NPs/PDMS composite films; b) SERS spectrum of thiram extracted from orange peel (1×10^{-4} M); SERS spectra of thiram extracted from apple peel

(down to 1×10^{-5} M) using Ag NPs/PDMS composite films. All spectra were recorded at 514 nm illumination wavelength.

Conclusions

In conclusion, Ag NPs/PDMS SERS composites were fabricated by self-assembly of organic Ag NP solutions at the air/solvent interfase. Model molecule 4–ABT was employed to test the SERS performance of fabricated transparent composites which exhibited high EF and good uniformity and batch to-batch reproducibility. Ag NPs/PDMS composites also showed excellent time stability and resistance to harsh conditions. The sticky nature of PDMS support was exploited to "paste" fabricated composites into contaminated fish skin and orange peel, leading to successful detection of food contaminant CV and pesticide thiram, respectively. As well as SERS detection by direct back illumination, detection by micro-extraction was demonstrated, which provided an alternative method of identification when matrices with strong background signals were analyzed.

Acknowledgements

This publication has emanated from research conducted with the financial support of the European Union H2020 project Nanorestart (646063) project and Science Foundation Ireland (SFI) under Grant Number SFI 16/RC/3918, co-funded by the European Regional Development Fund.

References

[1]. K.D. Osberg, M. Rycenga, G.R. Bourret, K.A. Brown, C.A. Mirkin, Dispersible Surface-Enhanced Raman Scattering nanosheets, *Adv. Mater.* 24 (2012) 6065–6070.

[2]. X. Yang, C. Gu, F. Qian, Y. Li, J.Z. Zhang, Highly sensitive detection of proteins and bacteria in aqueous solution using Surface-Enhanced Raman Scattering and optical fibers, *Anal. Chem.* 83 (2011**)**, 5888-5894.

[3]. A. Martín, C. Schopf, A. Pescaglini, J.J. Wang, J.J. D. Iacopino, Facile formation of ordered vertical arrays by droplet evaporation of Au nanorod organic solutions, *Langmuir* 30 (2014**)** 10206-12.

[4]. A. Martin, A. Pescaglini, C. Schopf, V. Scardaci, R. Coull, L. Byrne, D. Iacopino, Surface-Enhanced Raman Scattering of 4-aminobenzenethiol on Au nanorod ordered arrays, *J. Phys. Chem. C* 118 (2014) 13260-13267.

[5]. P.A. Mosier-Boss, Review of SERS substrates for chemical sensing, *Nanomaterials* 7 (2017) 142-172.

[6]. J. F. Betz, W.W. Yu, Y. Cheng, I.M. White, G.W. Rubloff, Simple SERS substrates: powerful, portable, and full of potential, *Phys. Chem. Chem. Phys*. 16 (2014**)** 2224-2239.

[7]. J. P. Singh, H.Y. Chu, J. Abell, R.A. Tripp, Y.P. Zhao, Flexible and mechanical strain resistant large area SERS active substrates, Nanoscale 4 (2012) 3410-3414.

[8]. G. Lu, H. Li, H. Zhang, Nanoparticle-coated PDMS elastomers for enhancement of Raman scattering, *Chem. Commun*. 47 (2011) 8560-8562.

[9]. W.Y. Wu, Z.P. Bian, W. Wang, J.J. Zhu, PDMS gold nanoparticle composite film-based silver enhanced colorimetric detection of cardiac troponin I, *Sens. Actuators B* 147 (2010) 298-303.

[10]. Y.H. Ngo, W.L. Then, W. Shen, G. Garnier, Gold nanoparticles paper as a SERS bio-diagnostic platform, *J. Coll. Inter. Sci.* 409 (2013) 59-65.

[11]. Y.H. Ngo, D. Li, G.P. Simon, G. Garnier, Gold nanoparticle-paper as a three-dimensional surface enhanced Raman scattering substrate, *Langmuir* 28 (2012) 8782-8790.

[12]. S. C. Tseng, C.C. Yu, D. Wan, H.L. Chen, L.A. Wang, M.C. Wu, W.F. Su, H.C. Han, L.C. Chen, Eco-Friendly Plasmonic Sensors: Using the Photothermal Effect to Prepare Metal Nanoparticle-Containing Test Papers for Highly Sensitive Colorimetric Detection, *Anal. Chem*. 84 (2012) 5140-5145.

[13]. D. He, B. Hu, Q. F. Yao, K. Wang, S.H. Yu, Large-scale synthesis of flexible free-standing SERS substrates with high sensitivity: electrospun PVA nanofibers embedded with controlled alignment of silver nanoparticles, *ACS Nano 3* (2009) 3993-4002.

[14]. C. L. Zhang, K.P. Lu, H.P. Cong, S.H. Yu, Controlled assemblies of Gold nanorods in PVA nanofiber matrix as flexible free-standing SERS substrates by electrospinning, *Small* 8 (2012) 648-653.

[15]. W. W. Yu, I.M. White, Inkjet printed Surface Enhanced Raman Spectroscopy array on cellulose paper, *Anal. Chem*. 82 (2010) 9626-9630.

[16]. Y. H. Ngo, D. Li, G.P. Simon, G. Garnier, Gold nanoparticle–paper as a three-dimensional Surface Enhanced Raman Scattering substrate, *Langmuir* 28 (2012) 8782-8790.

[17]. W.W. Yu, I.M. White, A simple filter-based approach to surface enhanced Raman spectroscopy for trace chemical detection, *Analyst* 137 (2012) 1168-1173.

[18]. A. Martín, J.J. Wang, D. Iacopino, Flexible SERS active substrates from ordered vertical Au nanorod arrays, *RSC Adv*. 4 (2014**)** 20038 – 20043.

[19]. C. Mathon, M. Duret, M. Kohler, P. Edder, S. Bieri, P. Christen, Multi-targeted screening of botanicals in food supplements by liquid chromatography with tandem mass spectrometry, *Food Chem.* 138 (2013) 709-717.

[20]. A. Masiá, M. Ibánez, C. Blasco, J.V. Sancho, Y. Picó, F. Hernández, Combined use of liquid chromatography triple quadrupole mass spectrometry and liquid chromatography quadrupole time-of-flight mass spectrometry in systematic screening of pesticides and other contaminants in water samples, *Anal. Chim. Acta* 761 (2013) 117-127.

[21]. L. Zhong, J. Yin, Y. Zheng, Q. Liu, X. Cheng, F. Luo, Self-Assembly of Au Nanoparticles on PMMA Template as Flexible, Transparent, and Highly Active SERS Substrates, *Anal. Chem.* 86 (2014) 6262-6267.

[22]. J. Chen, Y. Huang, P. Kannan, L. Zhang, Z. Lin, J. Zhang, T. Chen, L. Guo, Flexible and adhesive Surface Enhance Raman Scattering active tape for rapid detection of pesticide residues in fruits and vegetables, *Anal. Chem*. 88 (2016) 2149-2155.

[23]. N. Zhou, G. Meng, Z. Huang, Q. Zhou, X. Hu, A flexible transparent Ag-NC@PE film as a cut-and-paste SERS substrate for rapid in situ detection of organic pollutants, *Analyst* 141 (2016**)**

[24]. A. Shiohara, J. Langer, L. Polavarapu, L. Liz-Marzán, Solution processed polydimethylsiloxane/gold nanostar flexible substrates for plasmonic sensing, N*anoscale* 6 (2014**)** 9817-9823.

[25]. L. Rainville, D. Carolan, A. Coelho Varela, H. Doyle, D. Sheehan, Proteomic evaluation of citrate-coated silver nanoparticles toxicity in Daphnia magna, *Analyst* 139 (2014) 1678-1686.

[26]. K. Sugawa, Y. Tanoue, D. Tanaka, T. Sakai, Facile Phase Transfer of Gold and Au-Core/Ag-Shell Nanoparticles from Aqueous to Toluene Solution Using Alkylamine Molecules and Their Assemblies on Solid Supports, J*ap. J. Appl. Phys*. 50 (2011**)** 04DH14.

[27]. M. Sastry, A. Kumar, P. Mukherjee, Phase transfer of aqueous colloidal gold particles into organic solutions containing fatty amine molecules, *Colloids Surf. A* 181 (2001**)** 255-259.

[28]. X. Hu, T. Wang, L. Wang, S. Dong, Surface-Enhanced Raman Scattering of 4-aminothiophenol self-assembled monolayers in sandwich structure with nanoparticle shape dependence: off-surface plasmon resonance condition, *J. Phys. Chem. C* 111 (2007) 6962-6969.

[29]. M. Osawa, N. Matsuda, K. Yoshii, I.J. Uchida, Charge transfer resonance Raman process in surface-enhanced Raman scattering from p-aminothiophenol adsorbed on silver: Herzberg-Teller contribution, *Phys. Chem*. 98 (1994) 12702-12707.

[30]. J. R. Lombardi, R.L. Birke, A Unified Approach to Surface-Enhanced Raman Spectroscopy, *J. Phys. Chem. C* 112 (2008) 5605-5617.

[31]. S. Srivastava, R. Sinha, D. Roy, Toxicological effects of malachite green, *Aquatic Toxicol*., 66 (2004) 319-329.

[32]. Y.D. Shen, X.F. Deng, Z.L. Xu, Y. Wang, H.T. Lei, H. Wang, J.Y. Yang, Z.L. Xiao, Y. M. Sun, Simultaneous determination of malachite green, brilliant green and crystal

violet in grass carp tissues by a broad-specificity indirect competitive enzyme-linked immunosorbent assay, *Anal. Chim. Acta*, 707 (2011) 148-154.

[33]. M. V. Canamares, C. Chenal, R.L. Birke, J.R. Lombardi, DFT, SERS, and Single-Molecule SERS of Crystal Violet, *J. Phys. Chem. C* 112 (2008) 20295.

[34]. *Sittig's Handbook of Pesticides and Agricultural Chemicals* Second Edt., (2015) 769-838

[35]. F. Schulte, J. Mäder, L.W. Kroh, U. Panne, J. Kneipp, Characterization of Pollen Carotenoids with in situ and High-Performance Thin-Layer Chromatography Supported Resonant Raman Spectroscopy, *Anal. Chem*. 81 (2009) 8426-8433.

[36]. B. Sautea, R. Narayanan, Solution-based direct readout surface enhanced Raman spectroscopic (SERS) detection of ultra-low levels of thiram with dogbone shaped gold nanoparticles, *Analyst* 136 (2011) 527-532. https://doi.org/10.1039/C0AN00594K.

[37]. https://archive.epa.gov/pesticides/reregistration/web/pdf/0122red_thiram.pdf